

## A Design Optimization Study of Diffuser Shape in a Supersonic Inlet

S. Lim\*, D. H. Koh\*, S. D. Kim† and D. J. Song\*  
 Yeungnam University\*, Daegu University†

School of Mechanical Engineering, Yeungnam University, Republic of Korea  
 School of Automotive, Industrial and Mechanical Engineering, Daegu University†, Republic of Korea  
 wsns@yumail.ac.kr

Keywords: Supersonic inlet, Shape optimization

### Abstract

Optimum shape of Double-cone supersonic inlet is studied by using numerical methods. Double-cone intake shape is used for the design optimization study. And the total pressure recovery at the exit is used to assess the aerodynamic performance of the inlet.

### Introduction

The function of a supersonic inlet is to capture supersonic flow and efficiently to decelerate it in order to provide the engine with a sufficient mass flow rate of high total pressure subsonic flow. To achieve high performance, the inlet design must be optimized for the flight condition according to a set of constraints imposed by manufacturing restrictions and engine specifications.

A compression system of a supersonic inlet produces multiple oblique shock waves externally to reduce flow speed from freestream value, followed by normal shock wave near the inlet through which flow becomes subsonic. The interaction of a shock wave with a turbulent boundary layer yields large adverse pressure gradients causing rapid thickening and possible separation of the boundary layer. The diffuser shape in a supersonic inlet may be designed to minimize boundary layer thickness which is related to the shock/boundary-layer interaction<sup>1-2)</sup>.

### Numerical Method

#### Flowfields Analysis

The axisymmetric CSCM<sup>3)</sup> compressible upwind flux difference splitting Navier-Stokes code with the SST turbulence model is used to compute the inlet flowfields.

Table 1 shows test conditions for numerical analysis. Reynolds number based on cowl radius ( $R_c$ ) is about 650,000 and Mach number is 2.1. And cone angles are chosen by referring to Sedon and Goldsmith<sup>4)</sup> (Fig. 1)

Table 1 Test conditions

Re	650,000
Mach no.	2.1
Air Model	Perfect Gas
1 <sup>st</sup> cone angle ( $\delta_1$ )	20 deg
2 <sup>nd</sup> cone angle ( $\delta_2$ )	11.25 deg

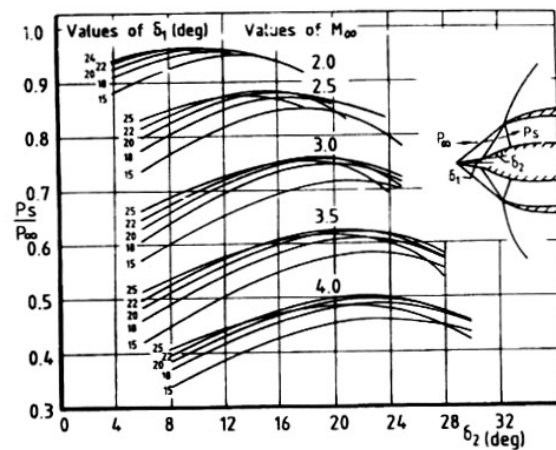


Fig. 1 Shock pressure recovery of double-cone intakes<sup>4)</sup>

Figure 2 shows the shape of Double-cone inlet used in this study. The shape from throat (1) to end of diffuser (2) is described by using Bezier-curve. And the control points of Bezier-curve are used for design variable.

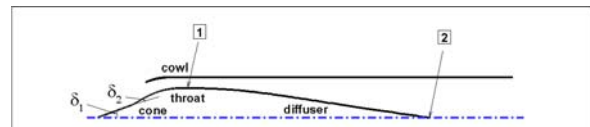


Fig. 2 Geometry of a supersonic inlet

Figure 3 shows grid system and boundary conditions. In this study, approximately 100,000 grid points are used for numerical analysis. At the inflow boundary of the inlet, all flow properties are fixed by external flow condition. The back pressure was specified as outflow boundary condition in order to generate normal shock waves within internal inlet flow field. The no-slip and adiabatic wall boundary conditions were imposed on the wall surfaces.

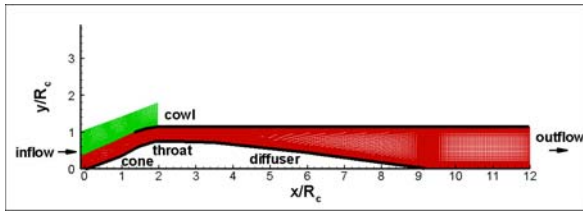


Fig. 3 Grid system and boundary conditions

### Bezier-curve<sup>5)</sup>

Control points of Bezier-curve can control the shape of curve. The starting and ending tangent vectors of Bezier-curve are determined by starting and ending control points and their neighbor control points. The  $k$  order Bezier-curve parametric function controlled by  $k+1$  control points is as follows.

$$Q(t) = \sum_{i=0}^k B_{i,k}(t) \times P_{i+1} \quad (1)$$

In Eq. (1),  $P_{i+1}$  mean control points.

Bernstein polynomials  $B_{i,k}(t)$  are as follow.

$$B_{i,k}(t) = \binom{k}{i} t^i (1-t)^{k-i} \quad (2)$$

$$\binom{k}{i} = \frac{k!}{i!(k-i)!}, \quad i = 0, 1, 2, \dots, k, \quad 0 \leq t \leq 1$$

### Response surface method (RSM)

The optimization procedure of using RSM includes selecting design domain, choosing sampling condition of design variable, analysis of object function, construction of response surface and analysis of variance.

Second order response surface function is described as following.

$$Y_{reg} = b_0 + \sum_{i=1}^m b_i X_i + \sum_{i=1}^m b_{ii} X_i^2 + \sum_{i=1}^{m-1} \sum_{j=i+1}^m b_{ij} X_i X_j \quad (3)$$

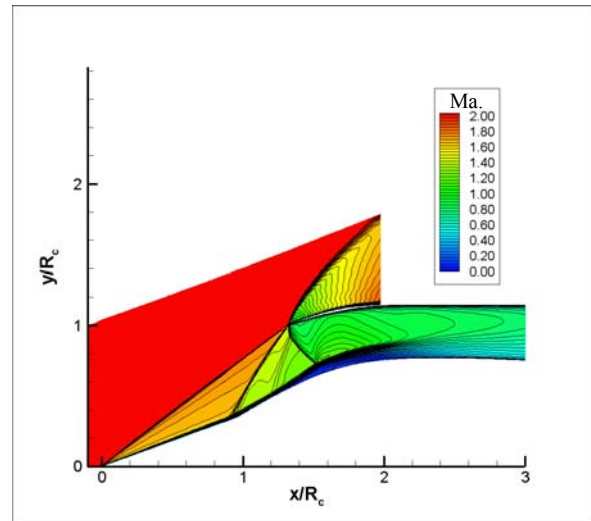
In Eq. (3),  $X_i$  means design variables and  $m$  means number of design variables. Coefficient  $b_i$  is determined by least square method.

## Results and Discussions

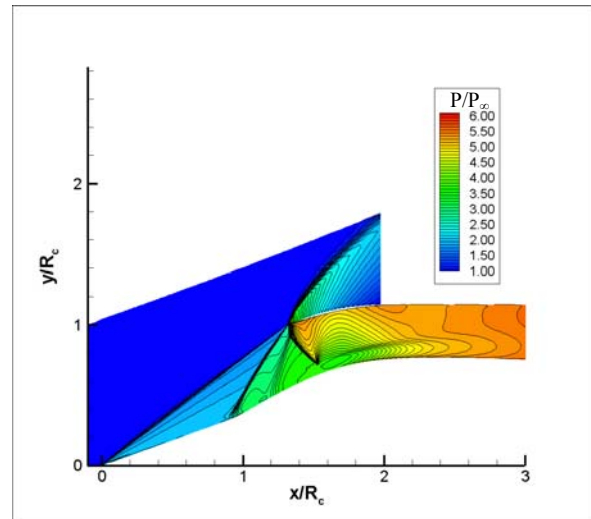
### The flow characteristics in a Double-cone inlet

In a high-speed supersonic aircraft configuration, a compression system produces an oblique shock wave externally to reduce flow speed from freestream value, followed by normal shock wave near the inlet through which flow becomes subsonic. The interaction of a shock wave with a turbulent boundary layer yields large adverse pressure gradients causing rapid thickening and possible separation of the boundary layer. The resulting shock/boundary layer interactions

may lead to total pressure losses and distorted boundary layer profiles that can seriously degrade engine performance.



(a) Mach number contours



(b) Non-dimensional static pressure contours

Fig. 4 Flow field near the double-cone and throat of a double-cone inlet (initial diffuser shape)

Figure 4 shows Mach number contours (Fig. 4 (a)) and non-dimensional static pressure contours (Fig. 4 (b)) near double-cone and throat which includes two oblique and a normal shock waves. It shows a severe distortion of pressure profile after the normal shock near the wall of second cone shape (on bottom surface), which is the shock/boundary layer interaction, and this shock boundary layer interaction induces very thick boundary layer in its downstream.

Diffuser shape

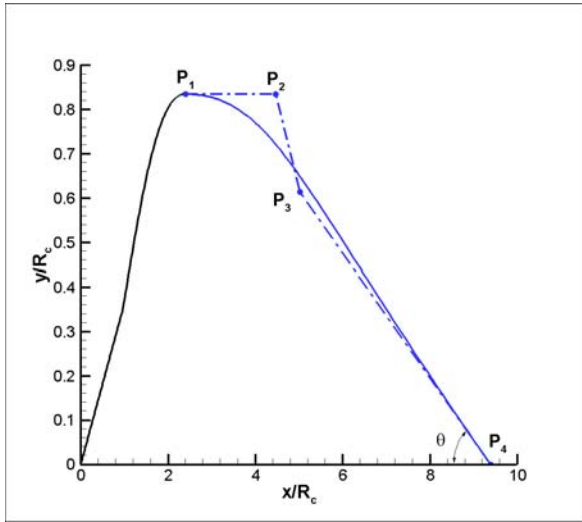


Fig. 5 Diffuser shape and control points of Bezier-curve

The diffuser shape is described by using Bezier-curve with four control points. The starting ( $P_1$ ) and ending ( $P_4$ ) control points are fixed, and the starting vector direction is fixed by horizontal direction as shown in Fig. 5. The length of starting ( $\overrightarrow{P_1P_2}$ ) and ending ( $\overrightarrow{P_4P_3}$ ) vectors are considered to design.

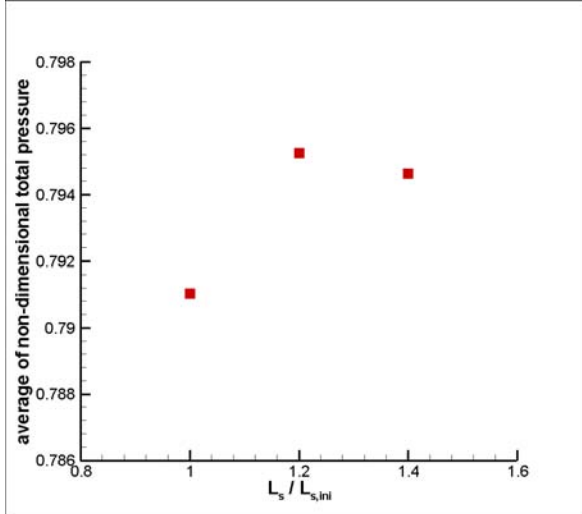


Fig. 6 A change of average non-dimensional total pressure according to the starting vector length

Figure 6 shows average non-dimensional total pressure at the aerodynamic interface plane (AIP) according to the change of starting vector length. Maximum average total pressure condition is shown near the  $L_s/L_{s,ini}=1.2$ .

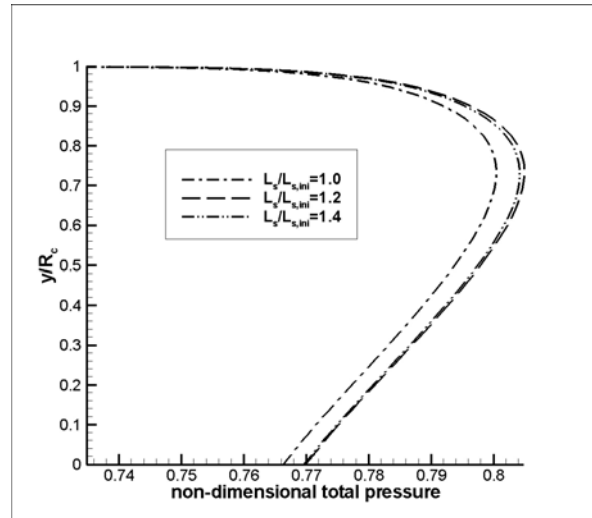


Fig. 7 Comparison of non-dimensional total pressure profiles among four different starting vector lengths

Figure 7 shows the comparison of non-dimensional total pressure profiles at the aerodynamic interface plane among three different starting vector length conditions. The magnitude of total pressure near the center ( $y/R_c=0$ ) of inlet and the maximum total pressure show some difference. But all of the cases show similar trend of non-dimensional total pressure profiles.

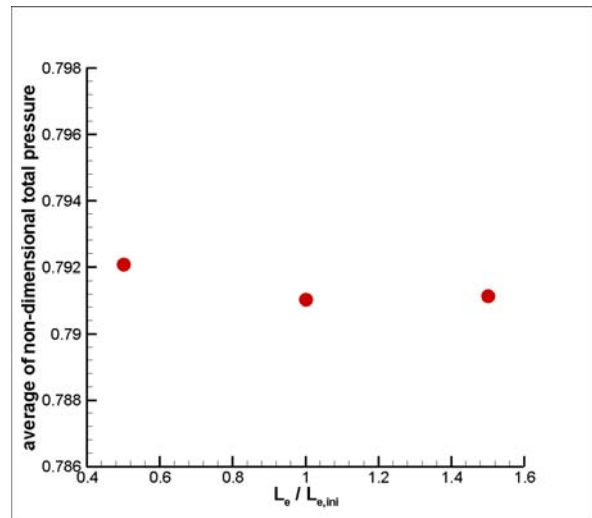


Fig. 8 A change of average non-dimensional total pressure according to the ending vector length

Figure 8 shows average non-dimensional total pressure at the aerodynamic interface plane (AIP) according to the change of ending vector length. In these cases, the change of average total pressure is very small (under 0.1%).

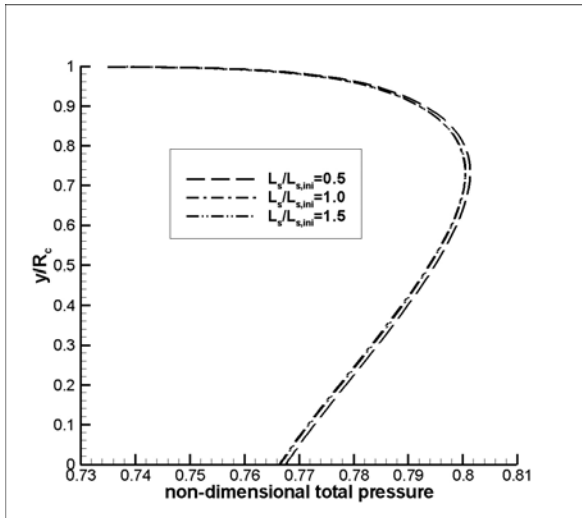


Fig. 9 Comparison of non-dimensional total pressure profiles among three different ending vector lengths

Figure 9 shows the comparison of non-dimensional total pressure profiles at the aerodynamic interface plane among three different ending vector length conditions. All of the cases show similar trend and magnitude of non-dimensional total pressure profiles.

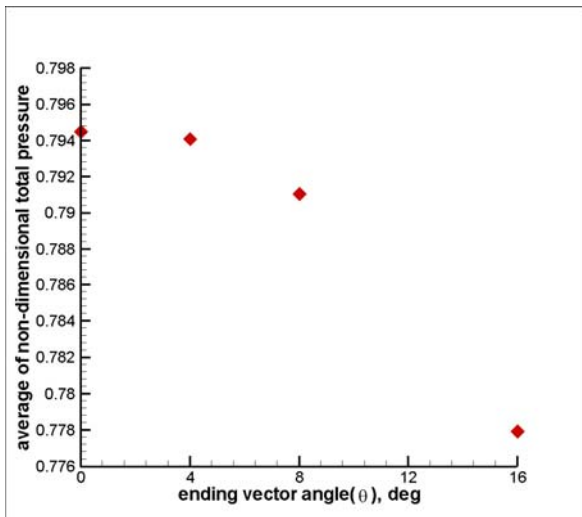


Fig. 10 A change of average non-dimensional total pressure according to the ending vector angle

Figure 10 shows average non-dimensional total pressure at the aerodynamic interface plane according to the change of ending vector angle( $\theta$ ). Average total pressure and ending vector angle show inverse proportional relationship. The maximum average total pressure is shown near the condition of 0 degree ending vector angle.

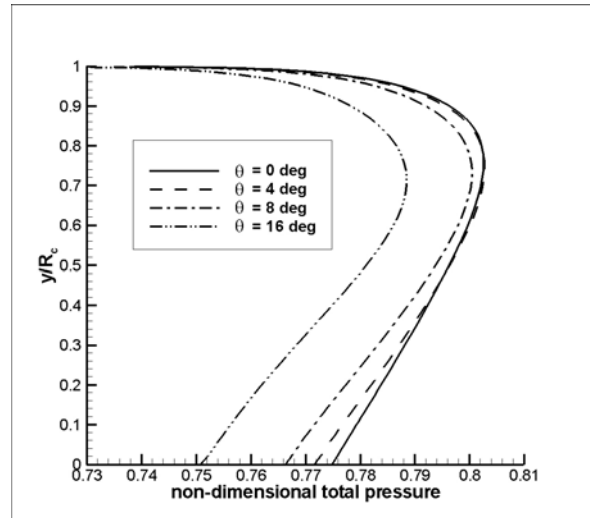


Fig. 11 Comparison of non-dimensional total pressure profiles among four different ending vector angles

Figure 11 shows the comparison of non-dimensional total pressure profiles at the aerodynamic interface plane among four different ending vector angle conditions. At the lower ending angle condition, the magnitude of total pressure profile is increased. But very low ending vector angle may cause weak strength at the end part of diffuser.

### Optimization

Response surface method is used for optimization study. Average non-dimensional total pressure at the aerodynamic interface plane is used for object function (Eq. 4). Starting vector length and ending vector angle of diffuser part are used at design variables (Eq. 5).

$$\text{Maximize: } f(X) = \frac{\overline{P_{t,e}}}{P_{t,\infty}} \quad (4)$$

$$\text{Variable : } X_1 = \frac{L_s}{L_{s,ini}}, \quad X_2 = \frac{\theta}{\theta_{ini}}$$

Table 2 Optimization results

	$X_1$	$X_2$	$f(X)$
Initial	1.0	1.0	0.791
Optimum(RSM)	1.29	0.12	0.799
Optimum(analysis)			0.796

Table 2 shows the optimum conditions of design variables and object function. The expected object functions by RSM and analysis results show some difference in object function, but both of them show the increase of inlet performance.

Figure 12 shows comparison of initial and optimized diffuser shape of double-cone inlet. Optimum diffuser shape has low angle of ending vector compared with initial diffuser shape, so it may affect the inlet performance. But the optimum shape does not show considerable improvement of inlet performance compared with initial shape.

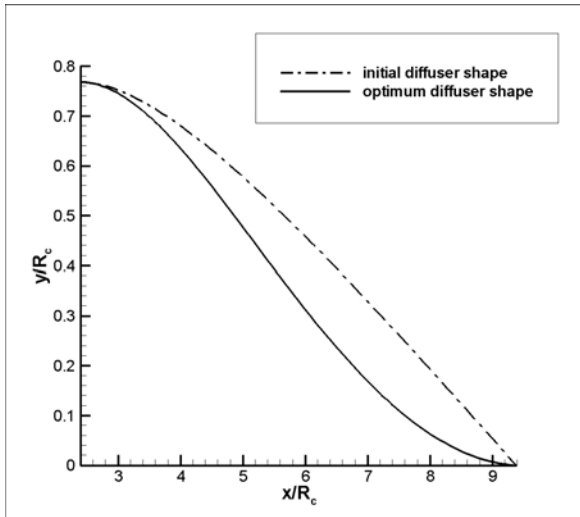


Fig. 12 Comparison of initial and optimum diffuser shape

Figure 13 shows comparison of Mach number contour between initial diffuser shape and optimum diffuser shape. In these results, it is difficult to find difference in flowfields between initial and optimum condition.

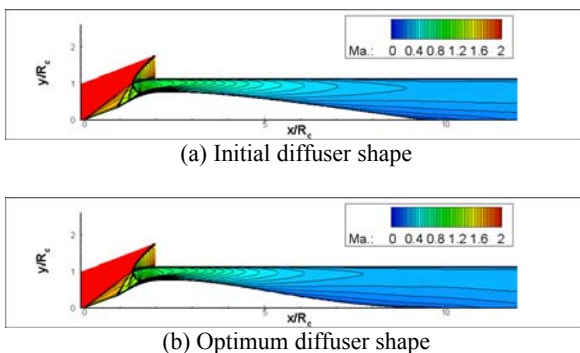


Fig. 13 Mach number contours

### Conclusion

The effect of diffuser shape of double-cone inlet is studied by using computational fluid dynamics. And the optimized diffuser shape has been obtained by using reaction surface method. Average total pressure at the aerodynamic interface plane is used for object function. The primary design variables of diffuser shape in using Bezier curve were starting vector length and ending vector angle were used for optimization study.

When the average total pressure is considered for object function, the starting vector length of diffuser shape has optimum condition, and lower ending vector angle of diffuser shape causes higher average total pressure. But the optimum shape does not show considerable improvement of inlet performance.

This work was supported by Defense Acquisition Program Administration and Agency for Defense Development under the contract UD070041AD.

### References

- 1) Kim, S. D., and Song, D. J., "The Numerical Study on the Supersonic Inlet Flow Field with a Bump," *Journal of Computational Fluids Engineering*, 2005, Vol. 10, No. 3, pp. 19~26.
- 2) Jung, S. Y., "Preliminary Design for Axisymmetric Supersonic Inlet using Conical Flow Solution and Optimization Technique," *KSAS*, 2006, Vol. 34, No. 9, pp. 11~19.
- 3) Lombard, C. K. et al., "Multi-Dimensional Formulation of CSCM an Upwind Flux Difference Eigenvector Split Method for the Compressible Navier-Stokes Equations", 1983, AIAA-83-1895,
- 4) Seddon, J. and Goldsmith, E. L., "Intake Aerodynamics", Second Edition, AIAA Education Series, VA., 1999
- 5) James D. Foley et al., "Introduction to Computer Graphics," Addison-Wesley Publishing Company, Inc., 1990